PERGAMON

Journal of Structural Geology 26 (2004) 113–126

JOURNAL OF STRUCTURAL GEOLOGY

www.elsevier.com/locate/jsg

Synchronous development of Type 2 and Type 3 fold interference patterns: evidence for recumbent sheath folds in the Allendale Area, Broken Hill, NSW, Australia

C.J. Forbes*, P.G. Betts, G.S. Lister

Australian Crustal Research Centre, School of Geosciences, Monash University, Melbourne, Australia

Received 12 July 2002; received in revised form 14 March 2003; accepted 28 March 2003

Abstract

Synchronous development of Type 2 and Type 3 fold interference patterns occur in the poly-deformed Broken Hill Inlier. The interference patterns have resulted from the superposition of recumbent F2 folds and ~N–S-oriented upright F3 folds. The synchronous development of Type 2 and Type 3 fold interference patterns is attributed to variation in the hinge of F2 folds by as much as 90°, suggesting the development of a regional-scale sheath-like fold geometry during D2. Overprinting relationships along the eastern limb of the Pap Synform suggests that it formed part of a recumbent fold hinge that was flattened during horizontal crustal shortening. This has resulted in the development of a modified Type 3 fold interference pattern. The results of this study show that the Type 2 and Type 3 fold interference patterns can develop during the same deformation event in an evolving orogen.

Keywords: Fold interference patterns; Sheath fold; Broken Hill; Australia; Proterozoic; Orogen

1. Introduction

The outcome of numerous studies of natural examples of fold interference patterns (e.g. Flin Flon, Manitoba, Canada; Stauffer and Mukherjee, 1971; Stauffer, 1988; Cantabrian Mountains, NW Spain; Julivert and Marcos, 1973), and numerical (e.g. Ghosh, 1970) and analogue (e.g. Watkinson, 1981; Ghosh et al., 1992, 1995; Grujic, 1993) models of fold superposition and the resultant geometries has been the recognition of four principle types of fold interference patterns. Ramsay (1962) and Ramsay and Huber (1987) classified the resultant geometries as Type 0 through to Type 3 interference patterns.

The identification of fold interference patterns in the field provides significant insight into the shortening history and kinematic controls of deformation within studied terranes. The geometry of superimposed fold generations to produce fold interference patterns is well understood (e.g. Ramsay, 1962; Thiessen and Means, 1980; Ramsay and Huber, 1987).

However, not all rocks deform in an ideal manner to produce ‘classic’ fold interference patterns, and map and outcrop patterns of fold interference patterns can easily become complex, as demonstrated by Thiessen (1986). Cross-sections through a fold interference pattern that result in the perfect representation of a Type 2 or Type 3 outcrop pattern are not always preserved. Thiessen (1986) showed that parallel cross-sections through refolded folds can produce a wide variety of patterns. Fold interference patterns that appear highly complex in outcrop can be described using simple refolding geometries, and vice versa; patterns that appear simple may be attributed to more complex refold histories. Therefore, it is important to attempt to observe the complete structure of an area and not make conclusions from observation of any one part of a structure.

The Palaeoproterozoic Broken Hill Block, central western New South Wales, Australia (Fig. 1) has undergone a complex deformation history during the Olarian Orogeny (1.60–1.58 Ga; Page et al., 2000) and Delamerian Orogeny (c. 520–490 Ma; Harrison and McDougall, 1981). This has resulted in the development of various tectonic models for the evolution of this area. There has been an emphasis on

* Corresponding author. Tel.: +61-3-9905-1127; fax: +61-3-9905-5062.
E-mail address: caroline@mail.earth.monash.edu.au (C.J. Forbes).

0191-8141/03/$ - see front matter © 2003 Elsevier Ltd. All rights reserved.
doi:10.1016/S0191-8141(03)00074-9

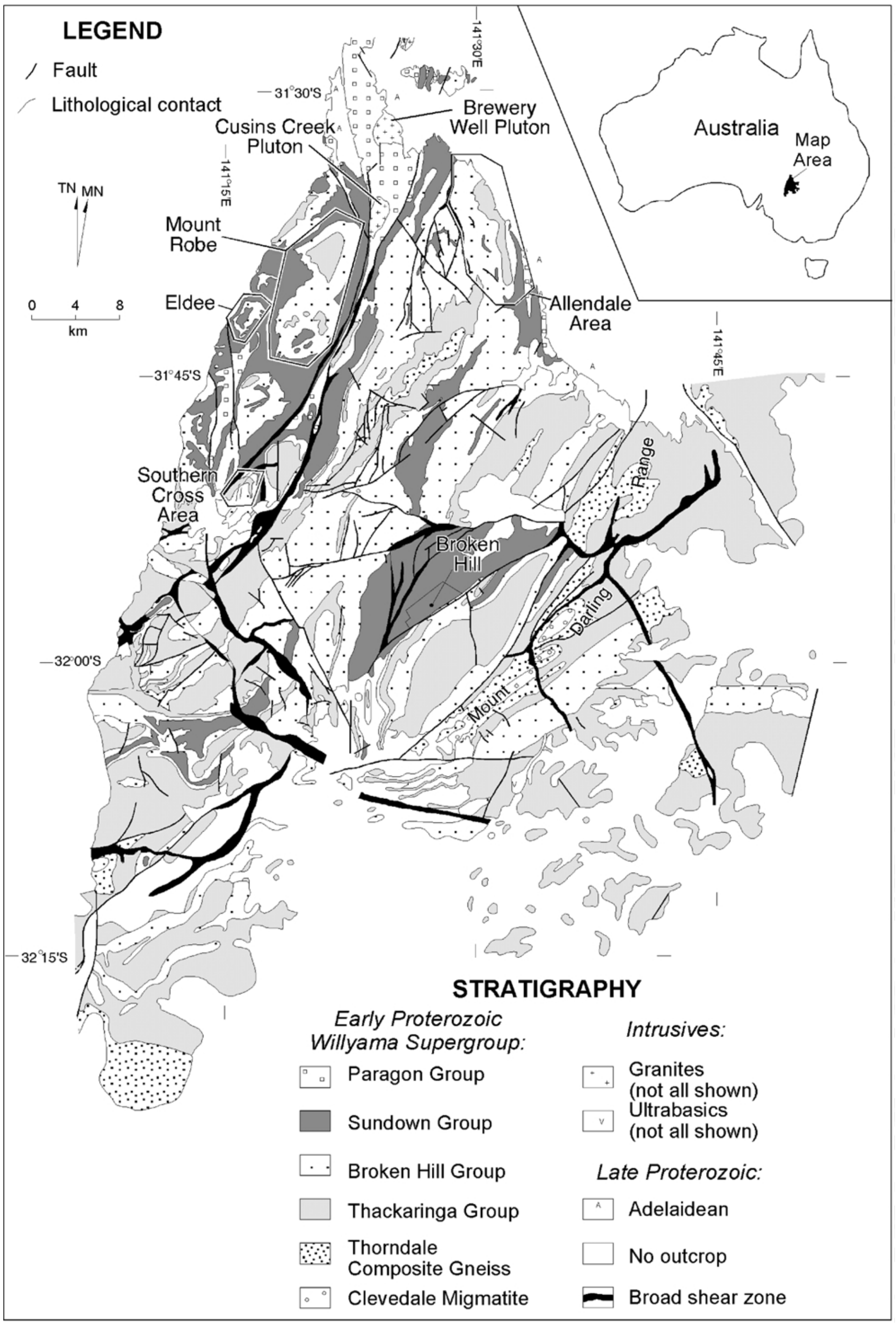

Fig. 1. Geological map of the Broken Hill Inlier showing the locality of the Allendale Area. The Eldee, Mount Robe and Southern Cross Areas are also shown (modified from Willis et al., 1983).

reconstructing stratigraphy and unfolding folds, but there have been few attempts to understand the relative timing of fabric forming events and their geometrical consequences.

Structural mapping conducted in the Allendale Area, located in the northern Broken Hill Block (Fig. 1), has revealed unusual fold interference patterns resultant from the superposition of upright, ~N–S-trending F3 folds over recumbent F2 folds. This deformation has resulted in the synchronous development of Type 2 mushroom–crescent and modified Type 3 convergent–divergent fold interference patterns regionally throughout the area. Overprinting relationships suggest a hidden hinge zone within the eastern limb of the fourth generation Paps Synform (Fig. 2). The resultant geometry is a modified Type 3 fold interference pattern where the hinge of the earlier fold generation (D2) has

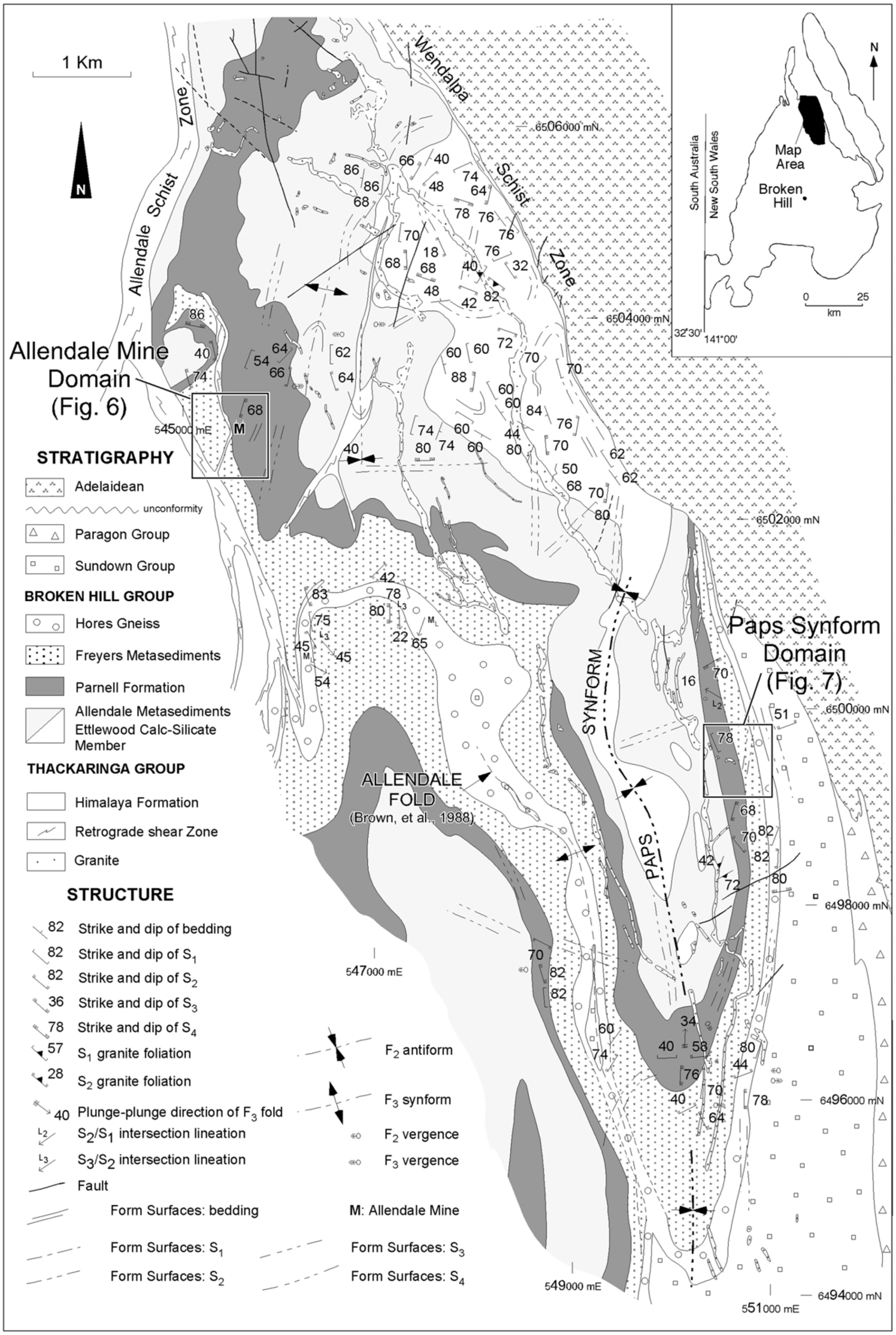

Fig. 2. Geological map of the Allendale Area showing the location of the Allendale Mine Domain and the Paps Synform Domain.

been flattened during D3 deformation, and now forms part of a straight limb of the F3 Paps Synform.

Synchronous development of Type 2 and Type 3 fold interference patterns and the discovery of an 'opened' recumbent fold raises the question of how these structural geometries could have developed. In this paper, we present structural analysis conducted in the Allendale Area. We focus on the development of fabrics and fold interference patterns associated with crustal shortening during the Olarian Orogeny.

2. Regional geology of the Broken Hill Block

The Broken Hill Inlier, western New South Wales (Fig. 1), comprises the polydeformed Early Proterozoic Willyama Supergroup (Fig. 3), which consists of metasedimentary rocks and metavolcanic rocks deposited within an intraplate rift basin (Stevens et al., 1988) between c. 1.73–1.64 Ga (Page and Laing, 1992; Donaghy et al., 1998; Nutman and Ehlers, 1998; Page et al., 2000). The Willyama Supergroup (Stevens et al., 1988) has been divided into several major stratigraphic groups (Fig. 3) based on detailed lithological mapping. The basal units of the Willyama Supergroup (Thackaringa Group and underlying packages; Fig. 3) comprise migmatitic gneiss and quartzofeldspathic rocks intercalated with psammopelites. These rocks have been dated, using U–Pb SHRIMP analysis of zircon within tuffaceous horizons, to have been deposited at c. 1.71 Ga (Love, 1992; Donaghy et al., 1998). Conformably overlying

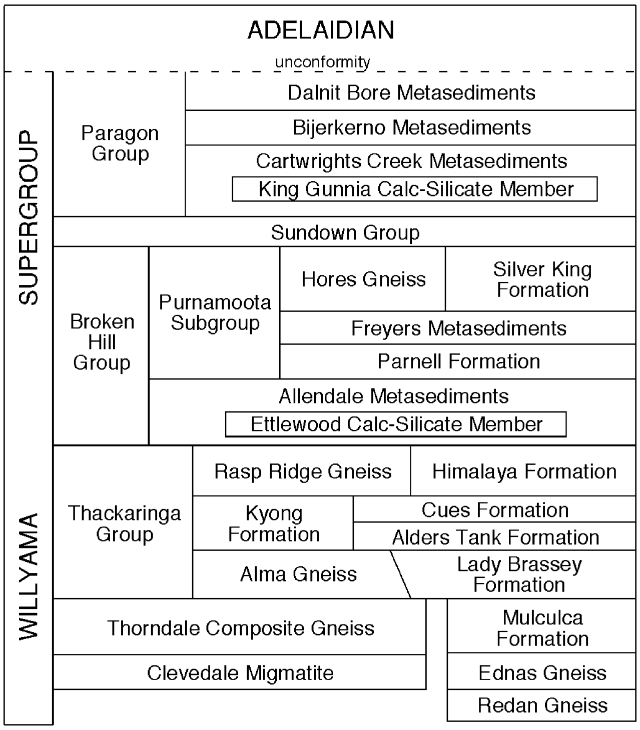

Fig. 3. Stratigraphic column of the Willyama Supergroup (Stevens et al., 1988).

these rocks is the Broken Hill Group (Fig. 3), which is a package of pelitic to psammopelitic metasediments and minor calc–silicate rocks, amphibolites and basic gneisses. These rocks have dominantly sedimentary protolith, although numerous quartz–feldspar–biotite gneisses have been interpreted partially as deformed volcanic rocks (e.g. Hores Gneiss; Stevens et al., 1988; Page and Laing, 1992) that were deposited by 1.69 Ga (Page et al., 2000). These are overlain by the Sundown and Paragon Groups (Fig. 3), which is a succession of psammite, pelite, calc–silicate rocks and graphitic phyllite and schist, interpreted to have been deposited during the post-extensional evolution of the basin (Willis et al., 1983; Walters, 1996). This sequence of rocks has a maximum depositional age of ~1.64 Ga (Page et al., 2000).

The basin was subsequently inverted during the Olarian Orogeny (c. 1.60–1.59 Ga; Page et al., 2000). Basin inversion involved complex polydeformation and high temperature–low pressure metamorphism, reaching upper amphibolite to granulite facies (e.g. Hobbs et al., 1984; Stevens et al., 1988). There have been several structural and tectonic interpretations for the evolution of the Broken Hill Inlier during the Olarian Orogeny (e.g. Marjoribanks et al., 1980; Hobbs et al., 1984; Stevens et al., 1988; Gibson, 2000; Page et al., 2000). Early structural analysis was based on regional-scale interpretations of stratigraphy and folds (e.g. Marjoribanks et al., 1980; Hobbs et al., 1984). Interpretations of the structural evolution include the development of an early generation of nappes of which the Broken Hill Inlier is part of an overturned limb of a regional-scale nappe (Marjoribanks et al., 1980). This nappe was interpreted to have been overprinted by several generations of upright folds during the Olarian Orogeny and during the Delamerian Orogeny (c. 520–490 Ma; Harrison and McDougall, 1981; Webster, 1996).

White et al. (1995) interpreted the regional geometry of the Broken Hill Inlier in the context of a high-temperature (mid-crustal level) fold and thrust belt that possibly originated under prograde metamorphic conditions. In this interpretation, the Broken Hill Inlier was divided into several discrete thrust slices that were interpreted to have undergone semi-independent structural evolutions. More recently, Gibson (2000) proposed that the earliest phases of deformation and associated high temperature–low pressure metamorphism resulted from significant extension in the middle crust. This extensional event has been interpreted to have occurred either during the early extensional phases of the basin c. 1.69 Ga (Gibson, 2000) or immediately prior to the Olarian Orogeny at c. 1.60 Ga (Venn, 2001). The extensional deformation may have been focussed in high-temperature shear zones, which developed in the middle groups of the Willyama Supergroup (Noble, 2000; Hills et al., 2001). Interpretations of an early extensional deformation phase in the Broken Hill Inlier are based on the development of a penetrative, lithology parallel foliation defined by high temperature-low pressure metamorphic assemblages and the absence of associated folding (Gibson, 2000). These shear zones have subsequently been folded during the Olarian Orogeny. Crustal shortening during the Olarian Orogeny was accompanied by high temperature–low pressure metamorphism, recumbent and upright folding and the emplacement of syn- to post-tectonic granites of the Mundi Mundi Suite (c. 1.59 Ga; Page et al., 2000) and pegmatites.

During the latest Neoproterozoic, the Broken Hill Inlier formed the basement to rift and passive margin successions of the Adelaidean cover sequences. These successions were deposited during continental break up of Australia and Laurentia (Powell et al., 1994). Basin inversion during the Delamerian Orogeny resulted in the development of a thin-skinned west-vergent fold and thrust belt (Paul et al., 2000). The influence of this orogenic event on Proterozoic basement is conjectural (e.g. Stevens, 1986; Webster, 1996).

3. Deformation history of the Allendale Region

Three fabric forming events have been identified within the Allendale Area. The first two fabrics are associated with upper amphibolite high-temperature–low pressure metamorphic conditions. The third fabric developed during lower-temperature metamorphism. The structural geometry of the area is dominated by fold interference of recumbent F2 folds superimposed by later ~N–S-trending upright F3 folds. Throughout the entire region, meso- and macroscopic scale outcropping Type 2 and Type 3 fold interference patterns suggest F2 folds were originally recumbent with variably oriented hinges.

3.1. First generation structures

The first generation fabric within the Allendale Area is a lithology parallel, penetrative but differentiated gneissic foliation that is particularly well developed within pelitic horizons. Within these pelitic units the S1 fabric is defined by muscovite (after sillimanite?) + biotite + sericite + quartz + feldspar (Fig. 4a and b). In the psammitic layers S1 is defined by elongation of quartz and feldspar aggregates and the alignment of minor muscovite and biotite laths. The mineral assemblage defining S1 suggests that it developed during amphibolite facies, high-temperature/low-pressure metamorphic conditions (e.g. Hobbs et al., 1984). The orientation of S1 is highly variable due to later refolding. A mineral lineation defined by muscovite, biotite, sericite (after sillimanite?) and occasional andalusite occurs in the plane of S1 (and compositional layering). Retrogression of these minerals to white mica is common. Mineral lineations are shallowly to steeply north- or south-plunging (Fig. 5a). This trend most likely reflects the dominance of north–south upright folding during later deformation. No folds have been recognised on the macro- or meso-scale.

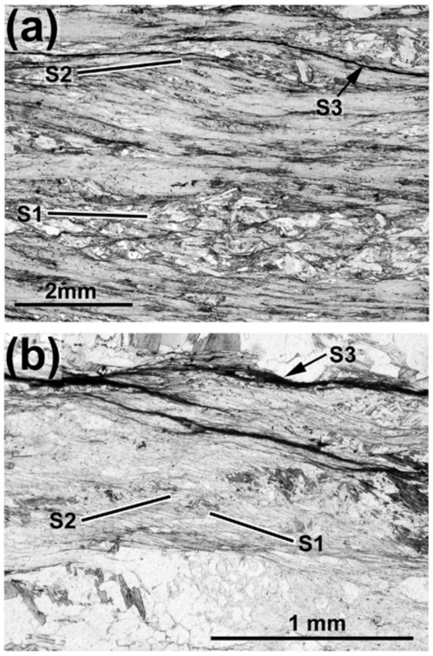

Fig. 4. Photomicrographs of rocks from the Allendale Area. (a) S1 within a pelitic unit showing quartz rich and mica rich domains. S2 is at a low angle to S1, is defined by biotite and crenulates the earlier fabric; (b) S1 is at a low angle to S3 and is difficult to distinguish. S2 is weakly preserved and is defined by biotite. S3 is defined by stylolites.

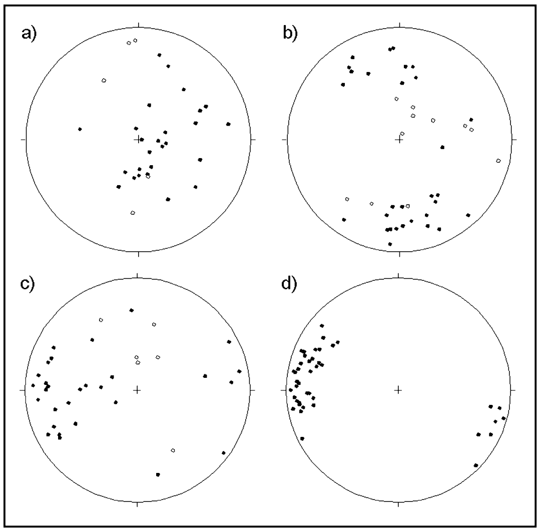

Fig. 5. Equal area stereographic projections presenting data from the Allendale Area. (a) Mineral lineations defined by muscovite, biotite, sericite (after sillimanite?) and occasional andalusite nodules. Filled circles: mineral lineations measured in the Allendale Mine Area; open circles: mineral lineations measured in the Paps Synform Domain; (b) filled circles: L2 intersections; open circles: F2 fold axes; (c) poles to S2 in the Allendale Mine Domain; filled circles: poles to S2 from F3 fold limbs; open circles: poles to S2 from F3 fold hinges; (d) poles to S3 in the Allendale Mine Domain.

3.2. Second generation structures

The second generation fabric is a weak to penetrative foliation that is characteristically spaced (on the millimetre scale) and is defined by muscovite and biotite in pelitic layers. In psammitic layers S2 is poorly defined, but when preserved is characterised by centimetre spaced elongation of biotite (Fig. 4a and b). This fabric is strongly differentiated and relatively weakly developed compared with S1. In hand specimen the S2 fabric is often defined by milky coloured wisps of retrogressed sillimanite.

Throughout the study area S2 is typically shallowly to moderately dipping (10–60°) and shows various relationships with compositional layering and S1. In the vicinity of the Allendale Mine (Fig. 2) S2 forms a composite foliation (Davis and Forde, 1994) with S1. On the eastern edges of the Inlier S2 is oriented at a high angle to S1 and compositional layering (Fig. 2). These relationships have been used to map larger scale F2 structures in the region. S2 is axial planar to F2 generation folds.

F2 folds are the oldest generation of folds recognised on a meso- to macroscopic scale in the study area. Their axial planes and fold axes are variably oriented due to later refolding (Fig. 2). They are characteristically tight to isoclinal and display similar fold styles. In the hinges of F3 upright folds, F2 folds are recumbent, and on the limbs of later fold generations they are typically shallowly to moderately inclined.

The intersection between S1 and S2, L2, is characterised by a millimetre spaced lineation defined by biotite and muscovite (after sillimanite?). The plunge of L2 is variable throughout the study area (Fig. 5b).

3.3. Third generation structures

The third generation foliation is approximately north–south to north–northeast-trending and is steeply dipping. S3 is a centimetre spaced fabric defined by dark stylolitic seams containing residual biotite and other insoluble opaque minerals (Fig. 4b). The microlithons between the stylolites contain crenulated S2 and S1 fabrics. On the limbs of many F3 folds, S3 is slightly oblique to compositional layering and S1 (Fig. 2) and can only be distinguished by its characteristic dark seams.

S3 is axial planar to open, upright folds that plunge variably approximately north or south (Fig. 2). Fold styles are typically similar with interlimb angles varying between 70 and 110°. This fold generation is responsible for the dominant north–south structural grain throughout the study area and the Broken Hill Inlier. The moderately north-plunging Paps Synform (Fig. 2) is a regional scale example of this generation of fold.

3.4. Fourth generation structures

A fourth deformation event was also identified locally. This event resulted in the development of approximately east–west-trending crenulations with steeply north or south dipping axial planes. Minor refolding and warping of earlier fold generations occurred during this event, but its overall effect on the regional structural grain is relatively minor, except for the development of local changes in F3 plunges. The timing of D4 is poorly constrained, and may have formed during post-Olarian Orogeny deformation.

3.5. Shear zones

Throughout the Allendale Area there are locally developed shear bands preserved within the metasediments. The locally developed shear bands are often very weak and have not fully developed into distinctive S–C fabrics. In other areas, the S–C fabrics are very well developed and associated with weak to strong mineral lineations. Two distinctive types of shear zones were observed in the Allendale Area. The earlier shear zones are higher metamorphic grade and have steeply dipping muscovite, biotite, sericite (after sillimanite?) mineral lineations. The early shear zones were predominantly observed around the Allendale Mine Area. Later retrograde shear zones (Fig. 2) are defined by phyllitic metasediments and contain abundant sericite, muscovite and chlorite. Mineral lineations in retrograde shear zones are shallowly to moderately dipping and are defined by muscovite and chlorite. These shear zones are not focussed on in this study as they were active late in the evolution of the Allendale Area, and are associated with localised retrograde metamorphism.

4. Structural domains

Two structural domains have been delineated based on differences in orientations of the overprinting fabrics, which are inferred to reflect the position or location within larger-scale regional F2 folds. The two domains are the Allendale Mine Domain (Fig. 6) and the Paps Synform Domain (Fig. 7a). These structural domains have been distinguished based on variations in the relationship between major fold related fabrics S2 and S3, as well as variations in the types of fold interference patterns developed.

4.1. Allendale Mine Domain

The Allendale Mine Domain (Fig. 6) is located in the northwestern portion of the study area. It is bound to the west by the greenschist facies Allendale Shear Zone (Fig. 6). The map pattern is dominated by the overprinting of F2 recumbent folds by north–south oriented F3 upright folds. F3 folds and their associated cleavages cause the dominant north–south structural grain (Fig. 6). The intensity of F3 folds is variable throughout the domain. This is partly attributed to strain variations across the domain as well as rheological contrast between the pelite and psammite dominated successions. For example, F3 folds in the pelitic

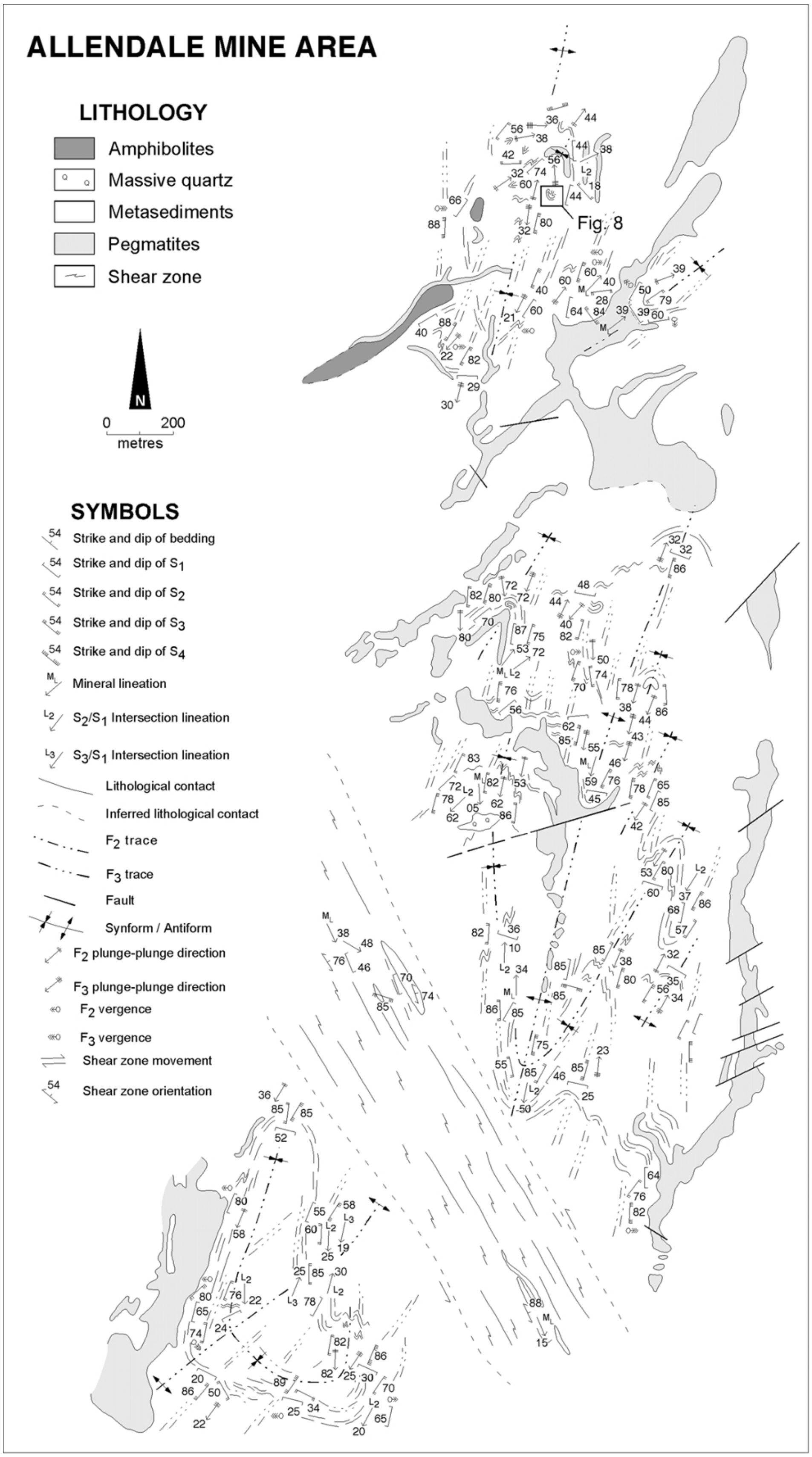

Fig. 6. Geological map of the Allendale Mine Domain. The outcrop location of the well-preserved Type 2 mushroom interference pattern (Fig. 8) observed in this area is shown.

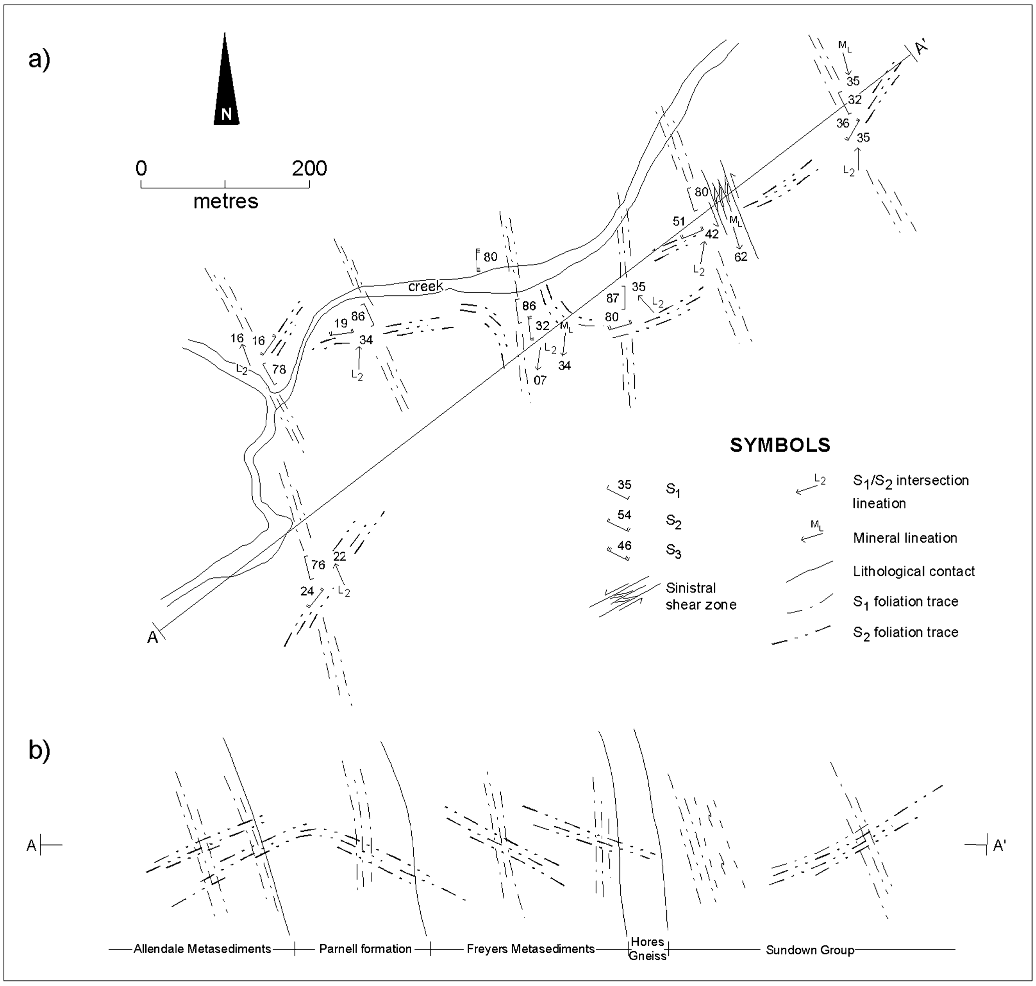

Fig. 7. (a) Geological map of the Paps Synform Domain; (b) creek section of the eastern Paps Synform limb showing S2 consistently at a high angle to S0/S1. Locality of the creek section is shown in Fig. 2.

units are generally tight to isoclinal, compared with open to close folds within psammitic units. Numerous pegmatites have intruded sub-parallel to the F3 axial plane throughout the domain.

Within the Allendale Mine Area, the S1 fabric is parallel to lithological layering. Locally S1 forms a composite fabric with S2, and is often slightly oblique to, or composite with, S3 on F3 fold limbs. The S2 fabric varies from shallow (10–30°) to moderate (50–70°) dipping across F3 fold hinges (Fig. 6). The S2 fabric is at a low angle (10–30°) to S3 (and S1) in F3 fold limbs; however, the angle between S2 and S3 is high in the hinge zones of F3 folds (up to 90°) (Fig. 5c and d). Meso-scale Type 2 fold interference patterns are locally developed within the hinge zones of F3 folds and have also been mapped in macro-scale (Fig. 6), suggesting F2 folds were originally recumbent within this domain, and that F2 and F3 generations were non-coaxial.

The meso-scale Type 2 mushroom interference pattern is best preserved in the northwest of the Allendale Mine Domain (Figs. 6 and 8). At this locality, S1 is folded sub-parallel to a quartzofeldspathic leucosome layer, highlighting the mushroom pattern (Fig. 8). F2 folds are tight to isoclinal and are doubly plunging due to later refolding during D3. On the eastern side of the outcrop, the F2 fold plunges moderately north–northeast, and on the western side, the F2 fold plunges shallowly east (Fig. 8). The F3 fold at this locality is approximately north–south-trending, steeply south plunging, open and upright. A well developed, steeply dipping crenulation cleavage (S3) has developed axial planar to the F3 fold. S3 crenulates S1 and S2. The F3 fold shows evidence of minor warping and is overprinted by weak F4 folding (Fig. 8).

Across the Allendale Mine Domain the S2 fabric is generally oriented at a low-angle ($<15°$) to S3 (Fig. 6). High angular relationships between these fabrics occur locally within the hinge zones of mesoscale F2 folds. We interpret this to indicate that the Allendale Mine Area is located on a limb of a regional scale F2 recumbent fold. Unfortunately younging criteria and facing are unreliable (on a regional-scale) due to the high-strain and high-grade metamorphism in the region. Therefore, we are unsure if the Allendale Mine Domain

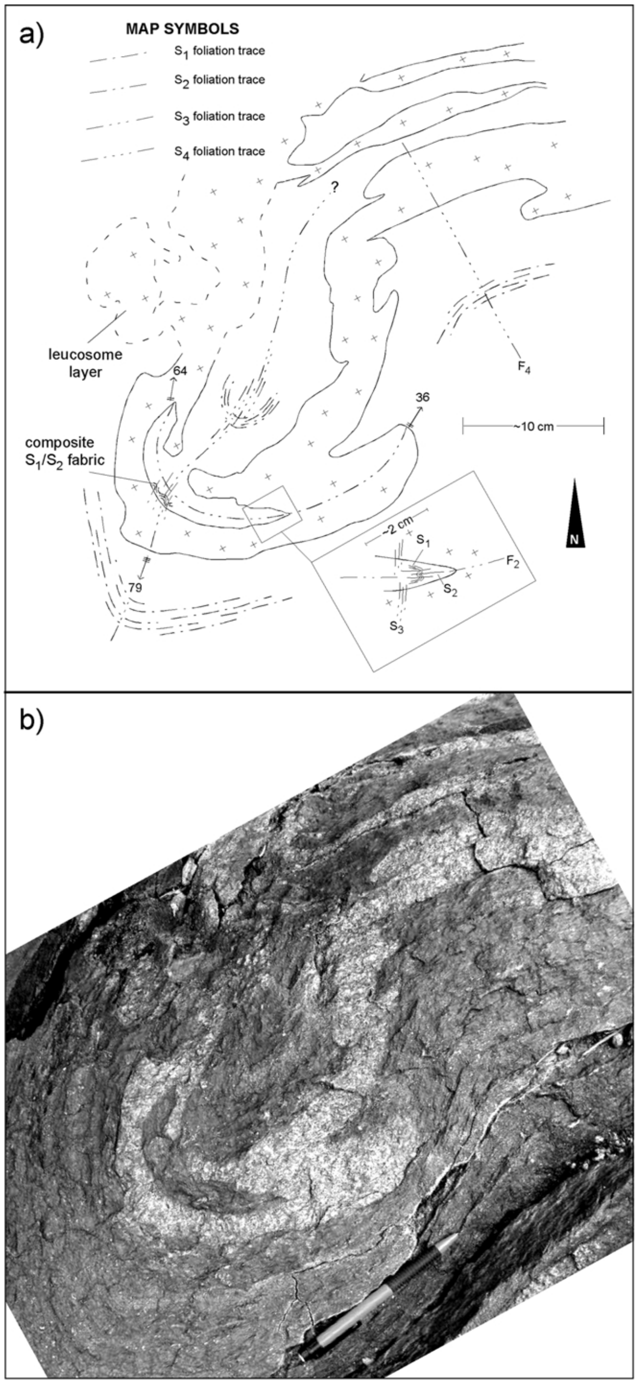

Fig. 8. (a) Sketch of the mushroom (Type 2) fold interference pattern observed in the Allendale Mine Domain. Axial traces of F2, F3 and F4 folds are shown. Locality of the outcrop is shown in Fig. 7; (b) Field photo of the same mushroom (Type 2) fold interference pattern sketched in (a). Pen is ~15 cm length.

is located on the upper or lower limb of a large-scale recumbent fold.

4.2. Paps Synform Domain

The Paps Synform domain (Fig. 7a) comprises the map-scale third-generation, upright, shallowly north-plunging Paps Synform, and numerous smaller scale F3 folds, which have north–northeast-trending axial surfaces and associated axial planar stylolitic cleavage. The F3 folds are truncated by numerous granitic dykes that are oriented subparallel to their axial plane.

In this domain the S1 foliation is parallel to lithological layering, and in part forms a fabric that has locally developed S–C shear planes. These shear zones are developed on the eastern limb of the Paps Synform where they extend for hundreds of metres along strike and are up to 30 m wide. This domain is distinguished from the Allendale Mine Domain because S2 is oriented at a high angle to S1 and lithological layering (Fig. 7). Typical angles between S1 and S2 vary between 45 and 90° (Fig. 7). The S2 fabric is generally shallowly (10–30°) to moderately (40–60°) dipping; however, in the hinge zones of meso- and map-scale F3 upright folds S2 is subhorizontal. This relationship between the fabrics is consistent over the entire domain, and suggests that the Paps Synform Domain is proximal to the hinge of a regional scale F2 recumbent fold. However, there is no obvious early recumbent hinge zones or folded lithology within the Paps Synform Domain (Fig. 7), suggesting the regional-scale F2 recumbent fold was ‘opened up’ during subsequent F3 folding (e.g. Fig. 9).

Refolding of S2 during subsequent deformation has resulted in the variations in orientation of the axial planes of F2 recumbent folds such that they are now shallowly to moderately inclined (Fig. 7). Assuming the high angular relationship (45–90°) between S1 and S2 is reflective of the original fabric relationships and has not been significantly modified during later deformation, this indicates a F2 fold hinge. The fold has been modified such that the north–south-trending limb of the Paps Synform now represents the remnant hinge zone of a F2 recumbent fold (Fig. 9). The geometry of this structure is inconsistent with that of a Type 2 or Type 3 fold interference pattern as proposed by Ramsay (1962). Instead, we propose that the geometry of the Paps Synform was formed in response to an episode of hinge ‘opening’ during the development of F3 upright folds (Fig. 9), producing a modified Type 3 fold interference pattern (Fig. 9).

5. Discussion

Analysis of fold interference patterns at individual localities does not necessarily constrain the regional-scale three-dimensional geometry since folds are not always cylindrical, and the hinge orientation can be highly variable. In addition, analogue model experiments have shown that the initial shape of the earlier fold generation can have significant influence on the resultant geometry after a second episode of deformation (e.g. Watkinson, 1981; Ghosh et al., 1992; Grujic, 1993). The variation in fold interference patterns between second and third generation folds from Type 3 in the Paps Synform to Type 2 in the

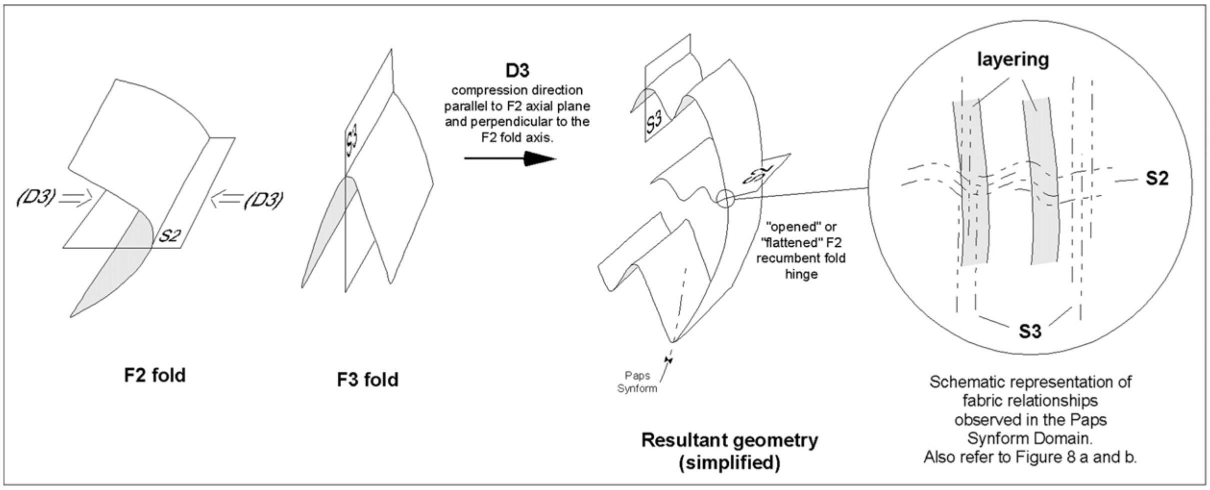

Fig. 9. Schematic diagram showing the mechanism of hinge flattening as the result of early open, recumbent folds being overprinted by later upright folds. A schematic representation of the fabric relationships in the Paps Synform Domain is shown in the enlargement.

vicinity of the Allendale Mine indicates that the fold hinge orientation of second generation folds change approximately 90° throughout the study area.

5.1. Synchronous development of Type 2 and Type 3 fold interference patterns

Any structural analysis of the Broken Hill Inlier/Allendale Area requires an explanation of regional variations in the types of fold interference patterns. In this study we have recognised Type 2 and Type 3 interference patterns between second and third generation folds. We interpret that these fold interference patterns developed synchronously, as the S2 and S3 foliations are defined by the same mineral assemblage and style of cleavage. We suggest that this results from overprinting of a highly non-cylindrical recumbent fold generation by regional upright folds. These changes in fold interference styles throughout the area have not been recognised, resulting in the development of simplified deformational histories and geometrical models (e.g. Brown et al., 1983; Willis, 1999).

Type 2 and Type 3 fold interference patterns can both develop by the superposition of upright folds over recumbent folds. The production of Type 2 or Type 3 fold interference patterns is dependent on the orientation of structural elements of the two interfering fold generations. In both cases, the angle between the fold axial plane of two fold generations is high. Type 2 fold interference patterns develop when the angle of the fold hinges of the two fold generations is high (i.e. non-coaxial generations of folds). Conversely, Type 3 fold interference patterns develop when the angle of the fold hinges of the two fold generations is low (i.e. coaxial fold generations) (e.g. Odonne and Vialon, 1987; Ramsay and Huber, 1987). Therefore, whether Type 2 or Type 3 fold interference patterns develop is dependant on the orientation of the hinges of the two superimposing fold generations.

Structural analysis within the Allendale Area show that F2 folds characteristically have an open, recumbent geometry, and F3 folds are upright, doubly plunging and tight to open. The axial traces of F3 folds are consistently ~N–S-trending across the Allendale Area, implying that the orientation of the axial trace of F2 fold generation must have initially varied as much as 90°.

We suggest that F2 meso-scale recumbent folds in the Allendale Area may have been part of a larger pre-existing structure with a sheath-like geometry (Fig. 10). If this macro-structure were overprinted by an upright folding event, Type 3 fold interference patterns would be produced on the flanks of the sheath-like fold where coaxial deformations occur. Within the nose of the sheath-like fold, non-coaxial deformation would occur so Type 2 fold interference patterns develop (Fig. 10).

The tectonic conditions under which a highly non-cylindrical recumbent (sheath) structure may have developed in the Broken Hill Block is conjectural. This geometry may develop as a sheath fold, sensu stricto, or may be a highly non-cylindrical nappe structure. Sheath folds develop under conditions of progressive simple shear and form as the result of high attenuation of deflections within layers in the shear zone (Minnigh, 1979; Cobbold and Quinquis, 1980; Alsop and Holdsworth, 1999). As a result, sheath folds tend to be considered as restricted to shear zones (e.g. Cobbold and Quinquis, 1980). Characteristic features of sheath folds include evidence of bulk simple shearing, strong stretching lineations, high strain zones and the development of strong mylonitic fabrics. Although all the indicators of sheath folding were not strongly developed or observed within the Allendale Area, evidence of sheath folding has been observed elsewhere in the Broken Hill Block. The Mount Robe (Venn, 2001) and Eldee (Hills et al., 2001) areas have been interpreted as large-scale sheath folds. Throughout the Broken Hill area, evidence of high strain zones has been observed. Wilson and Powell (2001)

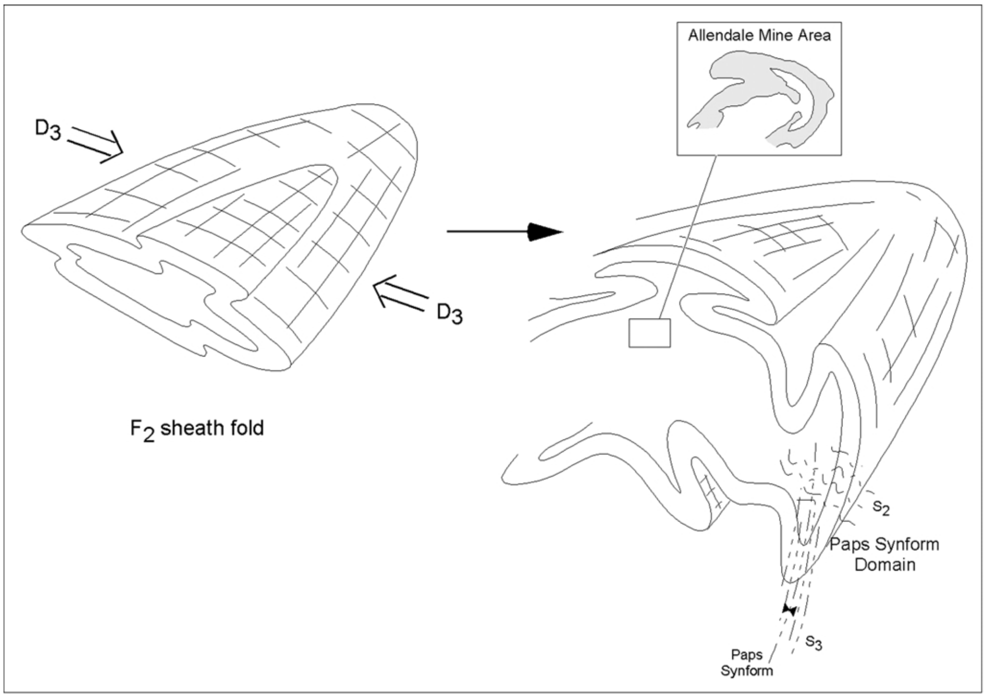

Fig. 10. Schematic representation of the 3D structural geometry of the Allendale Area. The early F2 sheath fold is shown to be overprinted by later upright folding during the D3 event to produce a complexly folded sheath structure. In the limbs of the sheath fold, Type 3 fold interference patterns are produced, whereas in the nose of the sheath fold, Type 2 fold interference patterns develop.

recognised early high-strain zones within the Southern Cross area (Fig. 1). These zones are characterised by a prominent foliation and sillimanite lineation, asymmetric extensional shear bands, tight to isoclinal intrafolial folds and pegmatites parallel to the foliation. To the north of the Broken Hill Block in the Euriowie area, a folded ductile high-temperature shear zone up to 200 m wide defined by a mylonitised granite was observed at the boundary of a granite gneiss (Alma Gneiss) and folded metasediments (Broken Hill Group) (Raetz et al., 2002). These high strain zones have not been placed in a regional-scale context. The presence of these shear zones throughout a large area of the Broken Hill Block suggests that the region was undergoing bulk shear strain during the Olarian Orogeny. If we have identified a sheath fold on the scale of 1–10 km in the Allendale Area, this implies that a large part of the crust underwent bulk simple shear during regional shortening.

Highly noncylindrical folds may also form during crustal-scale continental collision and overthrusting to develop fold and thrust belts and large-scale nappes. Large-scale sheath-like nappe structures have been described in the Western Gneiss Region of the Norwegian Caledonides as the result of the continental collision of Greenland and Scandinavia during the Silurian–Devonian (Vollmer, 1988). Nappe structures have been suggested as the dominant structural feature of Broken Hill geology for many years (e.g. Marjoribanks et al., 1980; Hobbs et al., 1984). However, the existence of these nappes has been highly debated due to the lack of small-scale nappe structures (e.g. Gibson, 2000) and the absence of identifiable detachment structures within the Broken Hill Block.

At the time of the Olarian Orogeny, the Broken Hill Block has been placed in a collisional setting as a result of a west-dipping subduction zone that lead to continental-scale collision between North America and Australian Proterozoic Cratons (Betts and Giles, 2001; Giles and Betts, 2001). This collision lead to the development of a N–S oriented orogenic belt along the eastern margin of Proterozoic Australia (Betts and Giles, 2001; Giles and Betts, 2001; Betts et al., 2002), which also included Georgetown (e.g. Withnall et al., 1997; Blewett et al., 1998), Mount Isa (Isan Orogeny; c. 1.60–1.50 Ga; Bell, 1983; Page and Sun, 1998; Betts et al., 1999, 2000; Lister et al., 1999; Giles and Nutman, 2002), the Northern Gawler Craton (Betts et al., 2002) and the Broken Hill Block (Olarian Orogeny). It is during the earliest stages of this orogeny that sheath folds or large-scale noncylindrical folds in the Allendale Area may have developed.

5.2. Hinge flattening in the Paps Synform Domain

Although the processes and mechanisms of recumbent fold generation are well understood (e.g. Ez, 2000), how these folds behave during subsequent deformation and crustal shortening has only been considered in the context of fold interference patterns. There has been little discussion of how the orientation of the hinge zones of recumbent folds behave during horizontal shortening. The original hinge orientation will have a marked effect on whether the hinge will be re-oriented (e.g. Cobbold and Watkinson, 1981; Watkinson and Cobbold, 1981; Odonne and Vialon, 1987) or will be flattened during later phases of folding/ deformation.

The shape of earlier fold generations has significant influence on the fold interference pattern produced subsequent to later deformation (Watkinson, 1981; Ghosh et al., 1992; Grujic, 1993). Watkinson (1981) used analogue modelling to show that refolding of tight to isoclinal folds results in folding of the hinge zone so that Type 2 mushroom interference patterns are produced. In contrast, if open, rounded folds are refolded, the hinge is not refolded, and Type 1 dome and basin structures are produced. Natural examples of this style of refolding can be observed in the Cantabrian Mountains in northwestern Spain, where tight antiforms were refolded to produce Type 2 interference patterns, and open synforms were refolded to produce Type 1 basin structures (Julivert and Marcos, 1973).

The refolding of initially open early fold hinges into open dome structures may be analogous to the Allendale Area where refolding may have resulted in the opening of a pre-existing F2 recumbent fold hinge that is now located on the eastern limb of the Paps Synform. The macroscopic F2 fold in the Allendale Area would have had an open, recumbent fold profile shape, which is similar to parasitic F2 recumbent folds observed in the Allendale Mine Area.

However, contradictory to Watkinson (1981), refolding of the earlier open fold in the Allendale Area did not produce a Type 1 dome and basin structure but a modified Type 3-like geometry (Fig. 9). Studies of the influence of the tightness of the earlier fold generation on the resulting geometry after superposition of later fold generations (e.g. Watkinson, 1981; Ghosh et al., 1992; Grujic, 1993) have focussed on early upright, open folds, where the superimposing fold generation had a compression direction parallel to the axial plane and the fold axis of the early generation fold (e.g. the Cantabrian Mountains, NW Spain; Fig. 3b; Watkinson, 1981) (Fig. 9). In contrast, the early folds in the Allendale Area are recumbent. The geometry of overprinting F3 folds shows that the shortening direction during this event was parallel to the axial plane, and *perpendicular* to the fold axis of F2 folds (Fig. 9). However, the suggestion that initially open folds may deform into open dome structures during subsequent deformation is valid. Therefore, it is suggested that during the D3 event in the Allendale Area, a macroscale recumbent F2 fold hinge was unfolded. The F2 fold hinge was incorporated into the limb of a large-scale F3 fold—now the eastern limb of the Paps Synform (Fig. 9).

6. Conclusions

Fold interference patterns can become extremely complex, and not all rocks behave in an ideal manner to produce 'classic' fold interference patterns. Fold interference patterns should be used in conjunction with detailed structural analysis and assessment of overprinting relationships to determine the true 3D geometry of an area.

The geometry of the Allendale Area is the result of fold interference of early D2 recumbent folds superimposed by later ~N–S-trending, upright D3 folds. Synchronous development of Type 2 and Type 3 fold interference patterns is interpreted to be the result of superposition of D3 upright folds over a large scale recumbent D2 sheath-like fold. A macroscale F2 hinge that has been opened by flattening and unfolding is preserved in the eastern limb of the Paps Synform. This F2 hinge zone can be recognised by the high angular relationship between the S2 and S3 fabrics in the area.

Acknowledgements

CF would like to acknowledge the pmd*CRC for support during part of the preparation of this manuscript. Catherine Spaggiari, Matt Noble and Quinton Hills are thanked for their assistance in the field, and Maurice Philips is thanked for his hospitality. David Giles, Laurent Aillieres, Barney Stevens, George Gibson and Maarten Krabbendam are thanked for helpful discussions. Constructive reviews and improvements to the manuscript from Barry Murphy, Djordje Grujic and Tom Blenkinsop were appreciated.

References

Alsop, G.I., Holdsworth, R.E., 1999. Vergence and facing patterns in large-scale sheath folds. Journal of Structural Geology 21, 1335–1349.

Bell, T.H., 1983. Thrusting and duplex formation at Mount Isa, Queensland, Australia. Nature 304, 493–497.

Betts, P.G., Giles, D., 2001. Proterozoic Australia and plate tectonics. GSA Abstracts with Programs 33, A-434.

Betts, P.G., Lister, G.S., Pound, K.S., 1999. Architecture of a Palaeoproterozoic rift system; evidence from the Fiery Creek Dome region, Mt. Isa Terrane. Australian Journal of Earth Sciences 46, 533–554.

Betts, P.G., Ailleres, L., Giles, D., Hough, M., 2000. Deformation history of the Hampden Synform in the Eastern fold belt of the Mt Isa Terrane. Australian Journal of Earth Sciences 47, 1113–1125.

Betts, P.G., Giles, D., Lister, G.S., Frick, L.R., 2002. Evolution of the Australian lithosphere. Australian Journal of Earth Sciences 49, 661–695.

Blewett, R.S., Black, L.P., Sun, S.S., Knutson, J., Hutton, L.J., Bain, J.H.C., 1998. U–Pb zircon and Sm–Nd geochronology of the Mesoproterozoic of North Queensland; implications for a Rodinian connection with the Belt Supergroup of North America. Precambrian Research 89, 101–127.

Brown, R.E., Willis, I.L., Ströud, W.J., Stevens, B.P.J., 1983. The relationship between mapped rock units and the stratigraphic subdivision of the Willyama Supergroup in key areas of the Broken Hill Block. The Aus.I.M.M. Conference, Broken Hill pp. 51–70.

Cobbold, P.R., Quinquis, H., 1980. Development of sheath folds in shear regimes. Journal of Structural Geology 2, 119–126.

Cobbold, P.R., Watkinson, A.J., 1981. Bending anisotropy: a mechanical constraint on the orientation of fold axes in an anisotropic medium. Tectonophysics 72, T1–T10.

Davis, B.K., Forde, A., 1994. Regional slaty cleavage formation and fold axis rotation by re-use and reactivation of pre-existing foliations; the Fiery Creek slate belt, North Queensland. Tectonophysics 230, 161–179.

Donaghy, A.G., Hall, M., Gibson, G.M., 1998. The Palaeoproterozoic Thackaringa Group: deposition, deformation and stratigraphy: Broken Hill Exploration Initiative. Abstracts of Papers Presented at the Fourth Annual Meeting in Broken Hill, October 19–21, pp. 17–20.

Ez, V., 2000. When shearing is a cause of folding. Earth Science Reviews 51, 155–172.

Ghosh, S.K., 1970. A theoretical study of intersecting fold patterns. Tectonophysics 9, 559–569.

Ghosh, S.K., Mandal, N., Khan, D., Deb, S.K., 1992. Modes of superposed buckling in single layers controlled by initial tightness of early folds. Journal of Structural Geology 14, 381–394.

Ghosh, S.K., Khan, D., Sengupta, S., 1995. Interfering folds in constrictional deformation. Journal of Structural Geology 17, 1361–1373.

Gibson, G.M., 2000. Tectonic evolution of the Paleoproterozoic Willyama Supergroup, Broken Hill: the early years: Broken Hill Exploration Initiative. Abstracts of Papers Presented at the May 2000 Conference in Broken Hill, pp. 45–47.

Giles, D., Betts, P.G., 2001. Proterozoic interactions between Australia and North America. GSA Abstracts with Programs 33, A-434.

Giles, D., Nutman, A.P., 2002. SHRIMP U–Pb monazite dating of 1600–1580 Ma amphibolite facies metamorphism in the southeastern Mt Isa Block, Australia. Australian Journal of Earth Sciences 49, 455–466.

Grujic, D., 1993. The influence of initial fold geometry on Type 1 and Type 2 interference patterns: an experimental approach. Journal of Structural Geology 15, 293–307.

Harrison, T.M., McDougall, I., 1981. Excess ^{40}Ar in metamorphic rocks from Broken Hill, New South Wales: implications for ^{40}Ar/^{39}Ar age spectra and the thermal history of the region. Earth and Planetary Science Letters 55, 123–149.

Hills, Q.G., Giles, D., Rosenbaum, G., Forbes, C., Lister, G.S., 2001. The Eldee Structure: a kilometre-scale sheath fold at the northwestern margin of the Broken Hill Block, N.S.W., Australia. Geological Society of Australia Abstracts 64, 81–82.

Hobbs, B.E., Archibald, N.J., Etheridge, M.A., Wall, V.J., 1984. Tectonic history of the Broken Hill Block, Australia. In: Kröner, A., Greiling, R. (Eds.), Precambrian Tectonics Illustrated, pp. 353–368.

Julivert, M., Marcos, A., 1973. Superimposed folding under flexural conditions in the Cantabrian zone, Hercynian Cordillera, N.W. Spain. American Journal of Science 273, 353–375.

Lister, G.S., O'Dea, M.G., Somaia, I., 1999. A tale of two synclines: rifting, inversion and transpressional popouts at Lake Julius, northwestern Mt. Isa Terrane. Australian Journal of Earth Sciences 46, 233–250.

Love, S., 1992. Possible ages and origins of some rocks of the Willyama Supergroup, New South Wales. Honours thesis, Australian National University.

Marjoribanks, R.W., Rutland, R.W.R., Glen, R.A., Laing, W.P., 1980. The structure and tectonic evolution of the Broken Hill Region, Australia. Precambrian Research 13, 209–240.

Minnigh, L.D., 1979. Structural analysis of sheath-folds in a meta-chert from the Western Italian Alps. Journal of Structural Geology 4, 275–282.

Noble, M., 2000. Geology of the Broken Hill Synform, N.S.W. MSc. thesis, Monash University.

Nutman, A.P., Ehlers, K., 1998. Evidence for multiple Palaeoproterozoic thermal events and magmatism adjacent to the Broken Hill Pb–Zn–Ag orebody, Australia. Precambrian Research 90, 203–238.

Odonne, F., Vialon, P., 1987. Hinge migration as a mechanism of superimposed folding. Journal of Structural Geology 9, 835–844.

Page, R.W., Laing, W.P., 1992. Felsic metavolcanic rocks related to the Broken Hill Pb–Zn–Ag orebody, Australia: geology, depositional age, and timing of high-grade metamorphism. Economic Geology 87, 2138–2168.

Page, R.W., Sun, S.S., 1998. Aspects of geochronology and crustal evolution in the Eastern Fold Belt, Mt Isa Inlier. Australian Journal of Earth Sciences 45, 343–361.

Page, R.W., Stevens, B.P.J., Gibson, G.M., Conor, C.H.H., 2000. Geochronology of Willyama Supergroup rocks between Olary and Broken Hill, and comparison to Northern Australia. Broken Hill Exploration Initiative: Abstracts of Papers Presented at the May 2000 Conference in Broken Hill, pp. 72–75.

Paul, E., Sandiford, M., Flöttmann, T., 2000. Structural geometry of a thick-skinned fold-thrust belt termination: the Olary Block in the Adelaide Fold Belt, South Australia. Australian Journal of Earth Sciences 47, 281–289.

Powell, C.M., Preiss, W.V., Gatehouse, C.G., Krapez, B., Li, Z.X., 1994. South Australian record of a Rodinian epicontinental basin and its mid-Neoproterozoic breakup (approximately 700 Ma) to form the palaeo-Pacific Ocean. Tectonophysics 237, 113–140.

Raetz, M., Forbes, C., Lister, G.S., 2002. Stratigraphic omission explained by discovery of a regional folded ductile shear zone in the Euriowie Block, NSW. Geological Society of Australia Abstracts 67, 185.

Ramsay, J.G., 1962. Interference patterns produced by the superposition of folds of "similar" type. Journal of Geology 60, 466–481.

Ramsay, J.G., Huber, M.I., 1987. The Techniques of Modern Structural Geology. Volume 2: Folds and Fractures, Academic Press, London, pp. 491–502.

Stauffer, M.R., 1988. Fold interference structures and coaptation folds. Tectonophysics 149, 339–343.

Stauffer, M.R., Mukherjee, A., 1971. Superimposed deformations in the Missi meta-sedimentary rocks near Flin Flon, Manitoba. Canadian Journal of Earth Sciences 8, 217–242.

Stevens, B.P.J., 1986. Post-depositional history of the Willyama Supergroup in the Broken Hill Block, NSW. Australian Journal of Earth Sciences 33, 73–98.

Stevens, B.P.J., Barnes, R.G., Brown, R.E., Ströud, W.J., Willis, I.L., 1988. The Willyama Supergroup in the Broken Hill and Euriowie Blocks, New South Wales. Precambrian Research 40/41, 297–327.

Thiessen, R., 1986. Two-dimensional refold interference patterns. Journal of Structural Geology 8, 563–573.

Thiessen, R.L., Means, W.D., 1980. Classification of fold interference patterns: a re-examination. Journal of Structural Geology 2, 311–316.

Venn, C.J., 2001. The geodynamic evolution of the Mount Robe and Mount Franks region, Broken Hill Australia: discovery of crustal-scale extensional shear zones and giant sheath folds. PhD thesis, Monash University.

Vollmer, F.W., 1988. A computer model of sheath-nappes formed during crustal shear in the Western Gneiss Region, central Norwegian Caledonides. Journal of Structural Geology 10, 735–743.

Walters, S.J., 1996. An overview of Broken Hill type deposits. In: Pongratz, J., Davidson, G.J. (Eds.), CODES Special Publication No. 1, New Developments in Broken Hill Type Deposits, University of Tasmania, pp. 1–10.

Watkinson, A.J., 1981. Patterns of fold interference: influence of early fold shapes. Journal of Structural Geology 3, 19–23.

Watkinson, A.J., Cobbold, P.R., 1981. Axial directions of folds in rocks with linear/planar fabrics. Journal of Structural Geology 3, 211–217.

Webster, A.E., 1996. Delamerian refolding of the Palaeoproterozoic Broken Hill Block. Australian Journal of Earth Sciences 43, 85–89.

White, S.H., Rothery, E., Lips, A.L.W., Barclay, T.J.R., 1995. Broken Hill area, Australia, as a Proterozoic fold and thrust belt: implications for the Broken Hill base-metal deposit. Transactions of the Institution of Mining and Metallurgy (Section B: Applied Earth Sciences) 104, B1–B17.

Willis, I.L., 1999. The Stratigraphic and Structural Context of the Broken Hill, Sundown and Paragon Groups, Willyama Supergroup, Broken Hill. Observations and Interpretations from Key Sequences at Yanco Glen and Euriowie. Volume 1: Report, ExSolutions Geoscience.

Willis, I.L., Brown, R.E., Ströud, W.J., Stevens, B.P.J., 1983. The Early Proterozoic Willyama Supergroup: stratigraphic subdivision and interpretation of high to low-grade metamorphic rocks in the Broken Hill Block, New South Wales. Journal of the Geological Society of Australia 30, 195–224.

Wilson, C.J.L., Powell, R., 2001. Strain localisation and high-grade metamorphism at Broken Hill, Australia: a view from the Southern Cross area. Tectonophysics 335, 193–210.

Withnall, I.W., Mackenzie, D.E., Denaro, T.J., Bain, J.H.C., Oversby, B.S., Knutson, J., Donchak, P.J.T., Champion, B.I., Wellman, P., Cruikshank, B.I., Sun, S.S., Pain, C.F., 1997. Georgetown Region. AGSO Bulletin 240, 19–116.